Available online at www.sciencedirect.com
ScienceDirect
Journal of Solid State Chemistry 180 (2007) 2409–2419
JOURNAL OF SOLID STATE CHEMISTRY
www.elsevier.com/locate/jssc

Aluminum speciation and thermal evolution of aluminas resulting from modified Yoldas sols

M. Dressler[a,*], M. Nofz[a], F. Malz[a], J. Pauli[a], C. Jäger[a], S. Reinsch[a], G. Scholz[b]

[a]*Federal Institute for Materials Research and Testing (BAM), Berlin, Germany*
[b]*Institute of Chemistry, Humboldt-University of Berlin, Berlin, Germany*

Received 7 March 2007; received in revised form 20 June 2007; accepted 20 June 2007
Available online 26 June 2007

Abstract

Aluminas resulting from sols prepared via a modified Yoldas procedure were studied with differential thermal analysis (DTA), differential thermal gravimetrie (DTG), ^{27}Al nuclear magnetic resonance (^{27}Al MAS NMR) and X-ray diffraction (XRD) concerning their thermal properties, aluminum speciation and phase content.

Hydrolysis of aluminum-*sec*-butoxide in aluminum nitrate solutions allowed to prepare stable sols with varying NO_3^-/Al molar ratios, solids contents and pH values. Resulting sols contained different aluminum species including also Al_{13} polycations. Sol preparation conditions also determined aluminum speciation in solid products obtained after thermal treatments of gels obtained from these sols. Al_{13} polycations and AlO_5 species were found to play an important role for thermally induced transformation from amorphous products via eta-Al_2O_3 to alpha-Al_2O_3. Intermediately formed eta-Al_2O_3 promotes the phase transformation to alpha-Al_2O_3.

Keywords: Alumina; Modified Yoldas sols; ^{27}Al nuclear magnetic resonance; Differential thermal analysis; X-ray diffraction

1. Introduction

Aluminas are of particular interest for many purposes. Either in the form of a bulk material or as a thin coating they can be used in applications such as catalysis [1], barrier coatings [2], abrasion resistance [3] and optics [4]. Reports about fiber drawing [5] can be found as well.

Different methods exist for synthesizing aluminas. Yoldas [6] described a method for preparing boehmite sols by hydrolyzing aluminum-*sec*-butoxide (ASB) in water at 75 °C, followed by peptization with HNO_3. The type of acid used [6], their concentration [6], the temperature during hydrolysis [7] and during gelling [8] have an influence on the resulting product. For example, Dynys et al. [9] followed Yoldas's procedure and reported that gelling of alumosols at 'room temperature' resulted in bayerite whereas gelling at 85 °C lead to 'poorly crystalline pseudoboehmite'. Alumina sols can also be prepared by increasing pH value of aluminum salt solutions by addition of a base [10–13]. A detailed introduction into the complexity of aluminum chemistry in solution is given in [14].

Many modifications of the above-mentioned procedures have been devised to change parameters such as pore size and surface area of resulting aluminas [1]. It is generally accepted that the way of preparation has a high influence on the type of alumina formed in sols and gels. In order to tailor resulting solid aluminas, not only information regarding the sol–gel transition but also the thermal transition behavior of the resulting gels/xerogels is vital.

This work presents data regarding thermal properties of aluminas resulting from sols prepared via a modified Yoldas procedure [15]. As shown in a previous work [16], these sols contain small particles, have an exceptional good long-term stability, Newtonian flow characteristic and a high optical transmission. Furthermore, Nofz et al. [17] showed that depending on pH these sols may contain Al_{13}

*Corresponding author.
E-mail address: martin.dressler@bam.de (M. Dressler).

0022-4596/$ - see front matter © 2007 Elsevier Inc. All rights reserved.
doi:10.1016/j.jssc.2007.06.018

polycations ($[AlO_4Al_{12}(OH)_{24}(OH_2)_{12}]^{7+}$) as a major constituent. Details regarding the structure of Al_{13} polycations can be found in [18,19]. The resulting alumina xerogels are of particular interest as Al_{13} polycations can be a precursor of both five-fold coordinated alumina [12] and probably eta-Al_2O_3 [13]. Five-fold coordinated alumina is being speculated to be a source of Lewis acidity [20]. Furthermore, eta-Al_2O_3 has a greater Lewis acidity than gamma-Al_2O_3 [21].

The aims of the present work are:

(i) to show the relations between aluminum speciation in sols and in xerogels produced thereof, and
(ii) to investigate the consequences of aluminum speciation for the thermally induced transformations of the xerogels.

2. Experimental

2.1. Materials

Twenty-four different alumina sols were prepared using diluted aluminum tri-*sec*-butoxide (ASB, 75 wt% ASB in *sec*-butoxide, Aldrich). ASB was weighed in a beaker and poured in one step into aqueous aluminum nitrate ($Al(NO_3)_3 \cdot 9H_2O$, puriss p.a., Merck) solution at 85 °C. NO_3^-/Al molar ratio was varied between $NO_3^-/Al \sim 0.2$ and $NO_3^-/Al \sim 2.2$. The upper limit ($NO_3^-/Al \sim 2.2$) was chosen because $NO_3^-/Al = 3.0$ would be a pure solution of aluminum nitrate. Sols with molar ratios ranging from 2.2 to 0.6 had a clear appearance [16]. A molar ratio of $NO_3^-/Al = 0.17$ resulted in sols with marked turbidity which gelled within days [16].

While stirred vigorously, the mixtures were kept at 85 °C for about 45 min. As a result of the addition of large amounts of ASB solution, a separate phase of *sec*-butoxide formed on top of the watery phase. No separate *sec*-butoxide phase was observed when preparing sols with much higher molar ratios than $NO_3^-/Al = 0.6$ (i.e., $NO_3^-/Al = 2.2$). To guarantee the same water and *sec*-butoxide evaporation regimes as for sols with $NO_3^-/Al = 0.6$, *sec*-butoxide (Merck) was added to the hot sols with $NO_3^-/Al = 2.2$ during synthesis. After cooling down to room temperature and removing the *sec*-butoxide the sols were reheated to 85 °C and left at that temperature for at least 30 min. To prepare more concentrated sols longer dwell times at 85 °C were necessary.

As described above, the desired amount of ASB for sol synthesis was weighed. Some of the ASB adhered to the walls of the beaker and as the remaining ASB residue may vary from synthesis to synthesis, the solids content, expressed as $c(Al_2O_3)$ in wt%, was determined for each sol in the following way. A defined amount of sol was dried at 85 °C in ambient air followed by a second drying step at 120 °C. The resulting xerogels were crushed in an agate mortar. Xerogels were thermally analyzed up to a maximum temperature of 1230 °C in a thermobalance (TAG24, Setaram). As a result, the Al_2O_3 content could be determined. The obtained number for Al_2O_3 content was used to calculate the actual molar ratio $n(NO_3^-)/n(Al)$ which will be abbreviated with NO_3^-/Al.

It should be noted that xerogels resulting from sols with high NO_3^-/Al molar ratio (above $NO_3^-/Al = 1.5$) show a marked hygroscopicity. All powders were stored at room temperature in tightly sealed receptacles which were placed in a desiccator. However, xerogel samples obtained after heating to 120 °C having parent sols with a molar ratio of $NO_3^-/Al \geqslant 1.5$ showed a marked hygroscopicity and still seemed to absorb water although being stored in a desiccator. The absorption of water affects the thermal evolution of xerogels as will be shown later. Samples which were subject to further analysis like XRD or ^{27}Al MAS NMR were not analyzed immediately but after aging for at least 1 month.

The thermal evolution of xerogels was studied at four temperatures: 120, 500, 850 and 1150 °C. Annealing to 500 and 850 °C was carried out in a muffle-type furnace (L9/SH, Nabertherm). For heat-treating samples at 1150 °C, another furnace (VMK 1800, Linn) was used. Samples were placed in corundum crucibles and heated with a heating rate of 10 K/min to the designated temperature at which they were held for 30 min.

Heat-treated samples had differing specific surface areas. Xerogels after preparation at 120 °C had surface areas in the range of 1 m^2/g whereas samples heat treated at 500 °C showed values ranging up to 230 m^2/g. Samples heat treated at 850 °C (1150 °C) had surface areas around 150 m^2/g (3 m^2/g).

Each xerogel sample will be presented with two parameters: (i) annealing temperature, and (ii) pH value of the parent sol. Thus, the following nomenclature is used in this work: a xerogel which has been heat-treated up to 120 °C and which originates from a sol with a pH value of 3.4, will be named x120-pH3.4.

2.2. Methods

2.2.1. ^{27}Al nuclear magnetic resonance spectroscopy (^{27}Al MAS NMR)

The spectra were acquired using a NMR spectrometer (14.1 T, Avance 600, Bruker BioSpin GmbH, Rheinstetten, Germany) with a 4 mm triple-resonance probe.

The ^{27}Al MAS NMR spectra of xerogels were obtained at 14.1 T (Larmor frequency of 156.3 MHz). Magic angle sample spinning (MAS) was applied using 4 mm zirconia rotors with a MAS spinning frequency of 13.5 kHz at room temperature. The spectra were acquired using 11° pulse (1 μs, 8 dB), a preacquisition delay of 6 μs, an acquisition time of 6 ms at a spectral width of 100,000 Hz, a relaxation delay of 20 s, and a total of 64 scans. Chemical shifts have been referenced using the octahedral ^{27}Al MAS NMR signal of yttrium aluminum garnet (YAG) at 0.6 ppm. All

^{27}Al MAS NMR signals presented in this work are scaled with respect to the strongest one for each sample measured.

2.2.2. Thermal analysis

Differential thermal gravimetric analysis (DTG) and differential thermal analysis (DTA) were recorded simultaneously in a thermobalance (TAG24) with 1600 °C equipment. Weighing error was $\Delta m = 0.01$ mg and error for temperature readings was $\Delta T = 5$ K. The test material (initial mass ~25 mg) was placed in an open Pt-crucible (100 µl). Samples were measured at a heating rate of 5 K/min in an argon plus air flow (volume flux flow rate ratio of argon and air was 3/4). The mass spectrometer (Quadstar 421, Balzers) for simultaneous analysis of evolved gases was coupled by a heated (120 °C) quartz glass capillary. Measurements were performed in MID modus. Evaluation of DTA data was carried out using software (Setsoft, Setaram) delivered from the thermobalance supplier.

2.2.3. X-ray diffraction (XRD)

X-ray diffraction measurements were performed on a diffractometer (FPM7, Seiffert, Freiberg, Germany) with Cu$K\alpha$ radiation. Phases were identified by comparison with the ICSD powder diffraction files.

3. Results

3.1. ^{27}Al MAS NMR spectroscopy

It is useful to distinguish three regions in ^{27}Al MAS NMR spectra. Acosta et al. [22] assigned the signals within the ranges (i) 50–80 ppm, (ii) 30–40 ppm, and (iii) −10 to 20 ppm to four-fold coordinated (AlO_4), five-fold coordinated (AlO_5) and six-fold coordinated (AlO_6) alumina, respectively.

Fig. 1 shows ^{27}Al MAS NMR spectra of xerogels which have been heated to different temperatures (120, 500, 850, 1150 °C). These samples result from sols with different pH values in the range between 2.7 and 4.9. The pH values are a result of differing NO_3^-/Al molar ratio whereas solids content ($c(Al_2O_3)$) was kept rather constant. The values for xerogels depicted in Fig. 1 ranged between $0.2 \leqslant NO_3^-/Al \leqslant 2.3$ and $6.0 \leqslant c(Al_2O_3) \leqslant 9.7$ wt%.

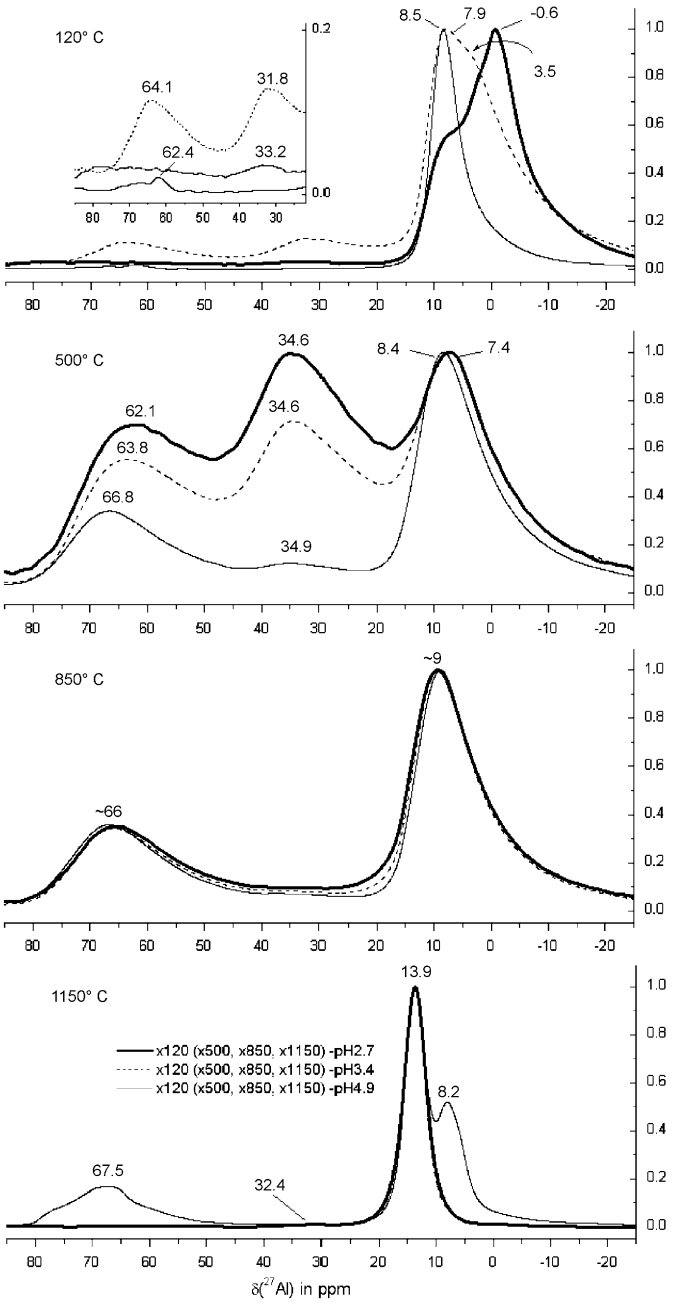

Fig. 1. ^{27}Al MAS NMR spectra of xerogels after heat treatment at different temperatures (120, 500, 850, 1150 °C) originating from sols with different pH values (2.7, 3.4, 4.9).

3.1.1. Samples heated to 120 °C

Irrespective of solids loading or NO_3^-/Al molar ratio, the following was found. A sol with an intermediate acidity of pH 3.4 (x120-pH3.4) lead to a xerogel, which after heating to 120 °C, contained distinct ^{27}Al MAS NMR resonances at 64.1, 31.8, 7.9 and 3.5 ppm. According to literature data summarized in Table 1, these resonances are ascribed to the central tetrahedron of the Al_{13} polycation (64.1 ppm), five-fold coordinated species (31.8 ppm), boehmite-like species (7.9 ppm), and six-fold coordinated species (3.5 ppm), which perhaps belong to Al_{13} polycations. The resonance at 3.5 ppm cannot unambiguously be assigned to AlO_6 groups incorporated in Al_{13} polycations. While in Ref. [11] peaks at 3.6 and 63.3 ppm were found when analyzing '$Al_{13}(SO_4)$', in Ref. [18], a resonance at 62.0 ppm caused by the central tetrahedron of the Al_{13} polycation was found but no peak in the region between 3.0 and 4.0 ppm. The resonances between 61.0 and 64.0 ppm detected in this work in xerogels after heating to 120 °C have not been assigned to transition aluminas as transition alumina formation is not expected to take place at annealing temperatures as low as 120 °C.

Table 1
Assignment of ^{27}Al MAS NMR resonances

Chemical shift, δ (^{27}Al) (ppm) Literature values		This work	Assignment	Sample
AlO_6				
		−0.6		x120-pH2.7
3.6	[11]	3.5	AlO_6 units perhaps belonging to Al_{13} polycations	x120-pH3.4
7.8	[25]	7.9, 8.5	Boehmite-like species	x120-pH4.9, x120-pH3.4, x120-pH2.7
9	[26]			
8.8	[27]			
10	[26]	7.4 to ~9	Transition aluminas	All samples after heat treatment at 500 °C and 850 °C, x1150-pH4.9
9.0	[27]			
6.29	[28]			
13.9	[27]	13.9	Corundum	All samples after heat treatment at 1150 °C
13.9±0.2	[29]			
AlO_5				
33	[12]	31.8–34.9	Five-fold coordinated aluminum species	x120-pH3.4, x120-pH2.7, all samples after heat treatment at 500 °C, residues in samples after heat treatment at 850 °C
36	[26]			
36–37	[27]			
38.0±1.0	[30]			
AlO_4				
62.0	[18]	62.4–64.1	Central tetrahedron of Al_{13} polycations	x120-pH3.4, x120-pH4.9
63.3	[11]			
67	[26]	62.1–67.5	Transition aluminas	All samples after heat treatment at 500 °C and 850 °C, x1150-pH4.9
68.8	[27]			
63.92	[28]			

Table 2
Composition (pH value, solids loading and NO_3^-/Al molar ratio) and TG-derived weight loss of xerogels analyzed in this work (C-series: high solids loading of parent sols $c(Al_2O_3)$~6.0–13.1 wt%, D-series: low solids loading of parent sols $c(Al_2O_3)$~0.2 wt%)

	Parent sol		Xerogel			
	pH	$c(Al_2O_3)$ (wt%)	NO_3/Al	Δm (wt%) RT–1230 °C	Δm[a] (wt%) 400–500 °C	Name
C-series	–	–	3.0	−87	−3	Aluminum nitrate
	2.4	9.3	1.6	−71	−4	
	2.7	4.7	2.3	−69	−4	x120-pH2.7
	3.4	9.7	0.6	−55	−6	x120-pH3.4
	3.8	7.9	0.5	−46	−9	
	4.9	6.0	0.2	−45	−9	x120-pH4.9
D-series	4.1	0.1	1.2	−51	−8	
	4.3	0.3	0.5	−37	−9	
			Plural	−18	−11	
			Disperal P2	−28	−8	

[a]Based on sample mass at 400 °C.

It can furthermore be seen in Fig. 1 that when reducing pH value of the parent sols below pH 3.4 or increasing pH value above 3.4, the resonances attributable to: (i) the central tetrahedron of the Al_{13} polycation (~63 ppm), (ii) AlO_5 (~35 ppm), and (iii) AlO_6 units perhaps belonging to Al_{13} polycations (3.5 ppm), become weaker or vanish. When increasing the pH value of parent sols above pH 3.4, the signal attributable to boehmite-like species (~8 ppm) remains the strongest resonance. Decreasing pH value to pH 2.7 (x120-pH2.7) leads to a ^{27}Al MAS NMR spectrum where six-fold coordinated species (−0.6 ppm) are the predominant component.

3.1.2. Samples heated to 500 °C

If annealing temperature is increased from 120 to 500 °C, xerogels show ^{27}Al MAS NMR resonances (Fig. 1)

attributable to transition aluminas (~64 and ~8 ppm, ref. Table 1) and five-fold coordinated species (~35 ppm). Irrespective of NO_3^-/Al molar ratio and solids loading of parent sols (ref. Table 2) the following pattern was observed: The higher the pH value of parent sols, the lower the relative signal height of signals at ~64 and ~35 ppm. All resonances attributable to six-fold coordinated species (−0.6 ppm) or AlO_6 units perhaps belonging to Al_{13} polycations (3.5 ppm), which have been observed in the samples heated to 120 °C are not detectable anymore after heating the samples to 500 °C.

3.1.3. Samples heated to 850 °C

As can be seen in Fig. 1, annealing xerogels at 850 °C leads to almost identical ^{27}Al MAS NMR spectra of all samples. The relative peak height of AlO_5 is ~0.1 in all samples. Hence, it can be surmised that still some aluminum is in five-fold coordination after heating to 850 °C as the signal at ~35 ppm does not disappear in any sample.

3.1.4. Samples heated to 1150 °C

The highest temperature to which xerogels were exposed to was 1150 °C. Thus, formation of alpha-Al_2O_3 was expected. A ^{27}Al MAS NMR spectrum of a reference alpha-Al_2O_3 sample (Alcoa) measured as well (spectrum not shown) exhibited only one sharp peak centered around ~13 ppm. As can be seen in Fig. 1, such a resonance is the only signal observable in samples originating from sols with a pH value of pH 2.7 and 3.4, i.e., x1150-pH2.7 and x1150-pH3.4. It is interesting to note that resonances attributable to transition aluminas (67.5 and 8.2 ppm) were found in sample x1150-pH4.9, whose parent sol observed the highest pH value compared to all other samples.

3.2. Thermal analysis

The samples whose thermal evolution was followed by ^{27}Al MAS NMR were also subject to DTA analysis whose results are shown in Fig. 2. It should be noted that xerogels prepared at 120 °C were analyzed via DTA. Aluminum nitrate and a commercial boehmite were also included into the investigations for comparison. Results shown in Fig. 2 are scaled with respect to sample mass in order to allow a direct comparison of peak heights. Two border cases of DTA curves can be seen in Fig. 2: (i) the DTA curve showing the thermal evolution of aluminum nitrate ($Al(NO_3)_3 \cdot 9H_2O$), and (ii) the DTA curve of a commercial boehmite (Disperal P2). All other depicted curves show either an aluminum-nitrate-like (x120-pH2.7, x120-pH3.4) or boehmite-like (x120-pH4.9) thermal evolution behavior. The general characteristics of the aluminum-nitrate-like samples are as follows: (i) in the temperature range well below 500 °C, a set of endothermic peaks appears which form a complex pattern, (ii) a very small exothermic signal at ~490 °C emerges (because of scaling reasons this signal is not distinguishable in each DTA plot shown),

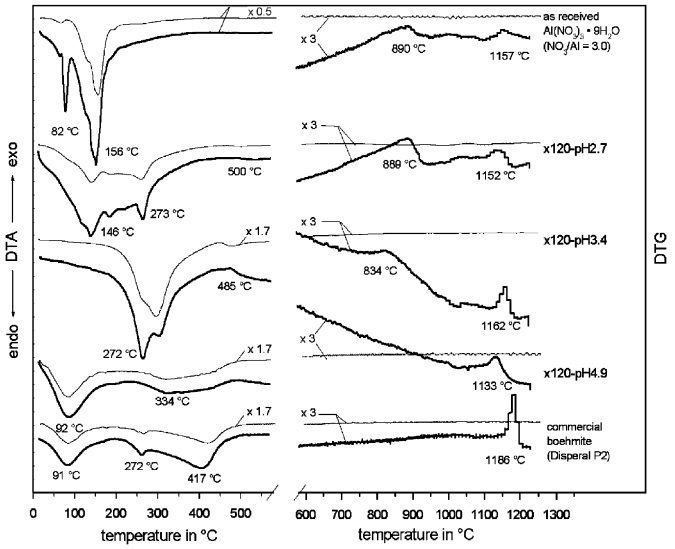

Fig. 2. DTA and DTG results for xerogels originating from sols with different pH values compared to commercial boehmite and aluminum nitrate. All curves are scaled to sample mass. Each scaling factor given refers to the scaling limits of the DTA/DTG plot of sample x120-pH2.7 at $T < 600$ °C.

(iii) between 800 and 900 °C another exothermic peak appears followed by (iv) an exothermic signal at temperatures higher than 1100 °C.

The DTA curve of the commercial boehmite (Disperal P2) and the boehmite-like sample (x120-pH4.9) has two distinct endothermic signals in the temperature range below 500 °C. No exothermic signal can be detected at ~490 °C or between 800 and 900 °C. The only exothermic signal appears at temperatures higher than 1100 °C.

The set of endothermic peaks below 500 °C in the aluminum nitrate-like xerogel samples (x120-pH2.7, x120-pH3.4) shows shifts towards lower temperatures with decreasing pH value of parent sols as can be seen if comparing samples x120-pH2.7 and x120-pH3.4. This effect should be related to water incorporation of the xerogel samples after preparation. As mentioned in the experimental section, xerogels having parent sols with a molar ratio equal or higher than $NO_3^-/Al = 1.5$ showed a marked hygroscopicity. Hence, sample x120-pH2.7 with a molar ratio of $NO_3^-/Al = 2.3$ (Table 2) was hygroscopic whereas sample x120-pH3.4 ($NO_3^-/Al = 0.6$, Table 2) did not show a tendency to absorb water. It was found that in these hygroscopic samples, the set of endothermic peaks (temperature range below 500 °C) exhibited a tendency to shift towards lower temperatures the longer they were stored. It is rather likely that these hygroscopic samples incorporated water from the ambient atmosphere although they were stored in a desiccator. This idea is supported by the finding that during DTG experiments, an increased mass loss was detected in aged xerogels compared to DTG results of freshly prepared ones. Although water content seems to have an influence on the position of the set of endothermic peaks below 500 °C, no significant influence of

water content on (i) the position of the exothermic peak between 800 and 900 °C and (ii) the last exothermic peak at ~1150 °C, could be observed.

The evolution of the DTG signals agrees well with the given DTA data as all major DTA signals at temperatures below 500 °C correspond with DTG signals. The only exception is the sharp endothermic signal at 82 °C in the DTA curve of aluminum nitrate which is caused by melting of the sample [24]. Only the barely recognizable peak at 79 °C seems to have a small corresponding DTG signal. It should be noted that the exothermic signal at about ~490 °C which has been recorded at xerogels whose parent sols had pH values of pH 2.7 and 3.4 (x120-pH2.7, x120-pH3.4), also corresponds to a DTG signal indicating a mass loss due to the release of nitric oxide. No distinct DTG peaks indicating a sudden mass loss above 500 °C are found in any xerogel sample. However, a constant but small (at most 3 wt%) mass loss above 500 °C is still measurable.

Table 2 summarizes the mass losses of xerogels being obtained from sols with different NO_3^-/Al molar ratios, different solids loadings, and different pH values within different temperature intervals. It is evident that reducing pH value leads to an increased overall mass loss between room temperature and 1230 °C. The comparatively lowest mass losses are found at two commercial boehmites, i.e., Disperal P2, which lost 28 wt% and Plural with a mass loss of 18 wt%.

The above reported mass losses are based on the sample mass at the beginning of the DTA analysis at room temperature. Some authors [23,31] use the mass loss in certain temperature intervals to verify the transformation process leading to boehmite. Table 2 also shows mass loss data between 400 and 500 °C based on the sample mass at 400 °C. A reverse trend compared to the overall mass loss between 500 and 1230 °C can be observed. Sols with low pH values lead to xerogels which have a lower mass loss within the 400–500 °C temperature interval compared to xerogels whose parent sols have a higher pH value.

Fig. 3 shows pH values of precursor sols in relation to NO_3^-/Al molar ratio and summarizes DTA peak temperatures of xerogels. The upper set of points shown in Fig. 3 represents the alpha-Al_2O_3 transformation temperature. The corresponding temperature of the peak between 800 and 900 °C is shown as well. No obvious trend between alpha-Al_2O_3 transformation temperature and NO_3^-/Al molar ratio or pH value of the parent sols can be seen. The observed scatter of the pH values results from the fact that sols having comparable NO_3^-/Al molar ratios but different solids loadings are shown simultaneously. The sols shown in Fig. 3 had solids loadings in the range $0.1 < c(Al_2O_3) < 11.6$ wt%. It is interesting to note that the exothermic peak between 800 and 900 °C decreases from ~900 to ~800 °C if lowering the NO_3^-/Al molar ratio of parent sols from 3.0 to ~0.4.

During DTA experiments, the evolving gases were analyzed via mass spectrometry (MS). Table 3 summarizes

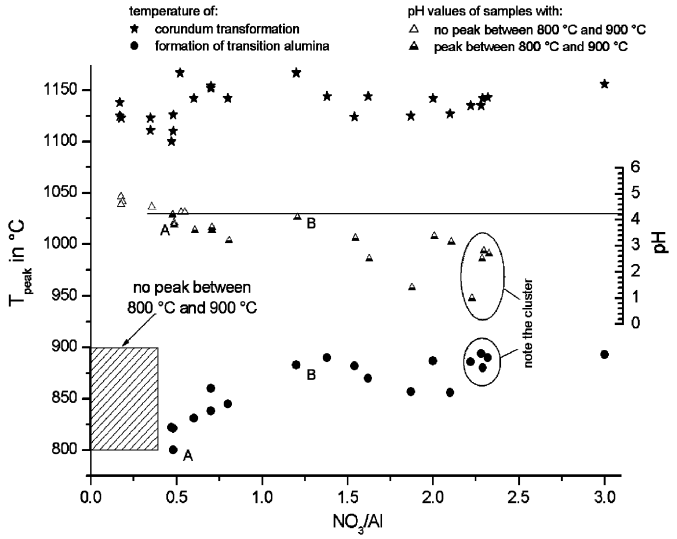

Fig. 3. Temperatures of transformations from transition alumina and temperatures of alpha-Al_2O_3 formation obtained from DTA results as a function of NO_3^-/Al molar ratio. Inset: pH value of parent sol for each xerogel sample depicted.

Table 3
Release temperatures of H_2O, NO_2 and CO_2 detected via mass spectrometry

	Peak position (°C)		
	H_2O	NO_2	CO_2
Aluminum nitrate	78 166	265 503 848	202
x120-pH2.7	177	258 510 875	239
x120-pH3.4	272	314 487 736	320
x120-pH4.9	110	387	294

the detected peak temperatures in the recorded MS curves for H_2O, NO_2 and CO_2. Alike to the findings for DTG, the detected MS peak temperatures correspond well to DTA peaks already shown in Fig. 2. As could have been suspected, the major endothermic reactions identified with DTA correspond to MS spectrometer peaks resulting from water desorption. The higher the pH value of the parent sols, the weaker the detectable MS signals for H_2O, NO_2 and CO_2. This finding agrees well with the mass loss data given in Table 2, as these xerogels also loose less mass between room temperature and 1230 °C. The small exothermic signal at ~490 °C shown in Fig. 2 corresponds to a small NO_2 signal. It is interesting to note that a small but discernible NO_2 signal can be found at temperatures above 700 °C in samples x120-pH2.7 and x120-pH3.4, which according to Fig. 2 show an aluminum-nitrate-like DTA pattern. A MS signal at such a comparatively high

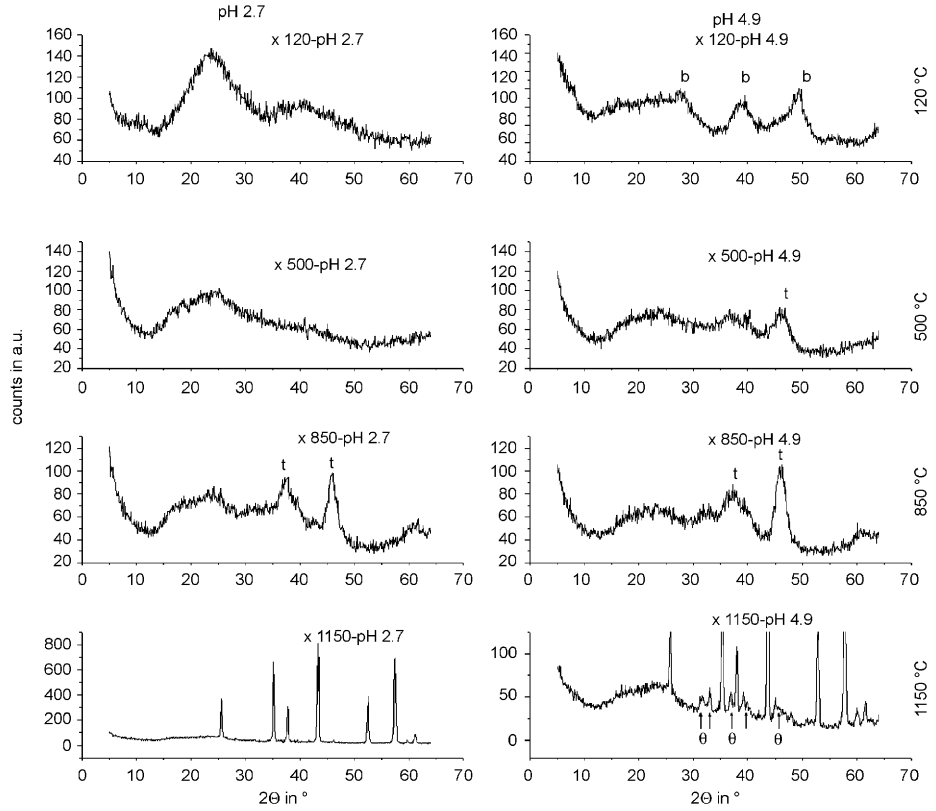

Fig. 4. XRD patterns of xerogels originating from sols having different pH values. 'b' indicates boehmite-like reflections, whereas 't' stands for unspecified transition alumina. 'Θ' denotes reflections of theta-Al_2O_3.

temperature was not found in sample x120-pH4.9 which observed a DTA transformation pattern according to a boehmite-like schema (Fig. 2).

3.3. XRD

Fig. 4 shows patterns of selected samples after different heat treatments. Sample x120-pH2.7 showed an aluminum-nitrate-like DTA transformation behavior, whereas sample x120-pH4.9 observed a boehmite-like DTA curve pattern (Fig. 2). Sample x120-pH2.7 shows the following thermal evolution regarding XRD results: The xerogel obtained after drying at 120 °C yields an amorphous pattern. Heat treatment at 500 °C results in a changed pattern which still can be interpreted as being indicative of an amorphous solid. After heat treatment at 850 °C, broad reflections of transition aluminas can be distinguished; these are indicated by a 't'. Final heating to 1150 °C obviously results in alpha-Al_2O_3 powder [32].

A different behavior can be observed for xerogel sample x120-pH4.9. The xerogel obtained after drying at 120 °C is not completely amorphous but shows some reflections of a poorly crystalline compound. The positions of these broad reflections of low intensity fit to those of boehmite [33], indicated by a 'b'. Both samples, those obtained after tempering at 500 °C (x500-pH4.9) and at 850 °C (x850-pH4.9), contain transition aluminas. The corresponding reflections are indicated by 't'. Heating sample x120-pH4.9 to 1150 °C did not enable a complete transformation to alpha-Al_2O_3 (Fig. 4, x1150-pH4.9). The XRD graph for this 1150 °C sample (x1150-pH4.9) is scaled here in a way to show that residues of theta-alumina still exist (labeled 'θ'). Additionally, it has to be mentioned that the reflections in x1150-pH4.9 caused by alpha-Al_2O_3 are only about 1/3 in intensity compared to those of the respective samples prepared from sols with a pH value of 2.7 (x1150-pH2.7).

The broad reflexes shown in Fig. 4 indicate the presence of 'nano-sized' particles which correspond to the very small particle size found in the parent sols. As was shown in a previous work [16], particle size in modified Yoldas sols ranges below 40 nm.

4. Discussion

In [17], it was shown that pH value of sols prepared according to the modified Yoldas procedure applied in this work determines the amount and stability of alumina species. Furthermore, these authors reported that increased temperature changes aluminum speciation in Al_{13} polycation containing sols. Hence, formation of xerogels via evaporation of dispersant is a complex process as not only temperature is increased but pH value changes constantly due to the loss of dispersant.

The results presented in Fig. 5 illustrate the dominating influence of pH value on phase transformation behavior of

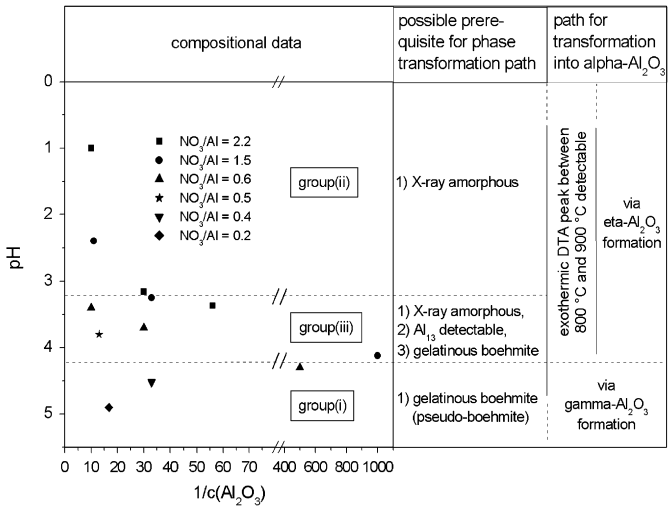

Fig. 5. Influence of pH value of parent sols on thermal evolution of resulting xerogels as well as possible prerequisites for thermal evolution involving either formation of gamma-Al_2O_3 or eta-Al_2O_3.

xerogels obtained from modified Yoldas sols. Using the data summarized in Fig. 5, as well as in the results part, xerogels in their state after heating to 120 °C can be divided into three groups:

Group(i), $pH \geqslant 4.2$: Sols with a pH value equal or greater than 4.2 yield 'boehmite-like' xerogels. After heating to 120 °C, XRD patterns attributable to some sort of boehmite were found. In conjunction with these XRD patterns, their ^{27}Al MAS NMR spectra show a distinct resonance at 8.5 ppm (Fig. 1, x120-pH4.9) which also is indicative of boehmite-like species ([25–27], ref. Table 1). No Al_{13} polycations were detected in these xerogels.

Group(ii), $pH < 3.2$: Most acidic sols regarded in this study (pH < 3.2) form 'amorphous' xerogels. After heating to 120 °C, samples were X-ray amorphous. Alike to group(i), these samples contained no Al_{13} polycations (Fig. 1, x120-pH2.7).

Group(iii), $3.2 \leqslant pH \leqslant 4.2$: Sols with pH values in the range between 3.2 and 4.2 result in 'intermediate' xerogels being X-ray amorphous but containing Al_{13} polycations, boehmite like species and five-fold coordinated aluminum (Fig. 1, x120-pH3.4).

This classification will be used in the following to discuss the typical properties and relationships between samples belonging to these groups.

4.1. Group(i)

As was shown in Fig. 2, xerogels having parent sols with a pH value above 4.2 have a DTA curve similar to that of commercial, well-crystallized boehmite. Similar DTA curves for boehmite can also be found in Refs. [26,34,35].

Different types of boehmite can be distinguished according to their XRD patterns and thermal behavior. According to Misra [38], aluminum hydroxides can generally be classified as either being crystalline or gelatinous. The latter of which can be subdivided into pseudo-boehmite and X-ray indifferent material. According to Nguefack et al. [39], '…the name pseudoboehmite is used for different solids resulting from different preparation conditions.' Their diffraction peaks are broadened compared to those of well-crystallized boehmite. Furthermore, pseudo-boehmite contains more water than well-crystallized boehmite (boehmite: 1.0 mol H_2O per mole Al_2O_3, pseudo-boehmite: 1.4 up to 2 mol H_2O per mole Al_2O_3, [40]).

An example for the DTA/DTG curves of a well-crystallized sample is given in Fig. 2 (commercial boehmite Disperal P2). This sample as well as the gelatinous (fibrillar) boehmite described by Souza Santos et al. [36] transforms via gamma-, delta- and theta-Al_2O_3 to alpha-Al_2O_3 (see also Ref. [37]). Regarding the nomenclature given by Misra [38], xerogels resulting from sols with a pH value above 4.2 (Fig. 5, group(i)) can be addressed as gelatinous material and more specifically as pseudo-boehmites as their DTA curves are boehmite-like (Fig. 2), but their XRD patterns are broad (Fig. 4) and a higher mass loss than commercial, well defined boehmite (Disperal P2) between room temperature and 1230 °C was recorded (ref. Table 2).

4.2. Group(ii)

Now the thermal behavior of the xerogels above summarized as group(ii) shall be considered. Tsuchida and co-workers [34,41] showed that extensive milling of crystalline gibbsite, bayerite and boehmite results in amorphization. In these amorphous samples, Tsuchida and co-workers [34,41] detected an eta-Al_2O_3 formation related exothermic DTA signal at ~800 °C. These findings agree with results reported by Steinike et al. [42]. Hence, one might ascribe the exothermic DTA signal between 800 and 900 °C detected in these Al_{13}-polycation-free xerogels belonging to group(ii) to eta-Al_2O_3 formation. According to Tsuchida and co-workers [34,41] and Steinike et al. [42], amorphous alumina is the prerequisite for eta-Al_2O_3 formation. This prerequisite is fulfiled as xerogels summarized in group(ii) are X-ray amorphous up to 500 °C (Fig. 4, x120-pH2.7, x500-pH2.7). Furthermore, after heating to 500 °C ^{27}Al MAS NMR spectra show a major resonance at ~35 ppm (Fig. 1, x500-pH2.7). This resonance is indicative of AlO_5 which usually is found in amorphous aluminas [12,26,27,30].

4.3. Group(iii)

Xerogels belonging to group(iii) (Fig. 5), i.e. whose parent sols have a pH value between 3.2 and 4.2, have many similarities to group(ii) samples. Both xerogel types show the eta-Al_2O_3 formation related exothermic DTA peak between 800 and 900 °C. Both group(ii) and group(iii) xerogels were X-ray amorphous after heating to 500 °C (X-ray results for group(iii) samples not shown), and the

corresponding ^{27}Al MAS NMR spectra also show the presence of five-fold coordinated alumina (Fig. 1, x500-pH3.4). In addition, the ^{27}Al MAS NMR spectra after heating to 1150 °C were identical between group(ii) and group(iii) samples.

Nevertheless, group(iii) xerogels are discussed separately for the following reasons. In contrast to group(ii) samples, group(iii) xerogels showed — after heating to 120 °C — ^{27}Al MAS NMR resonances (Fig. 1, x120-pH3.4) attributable to Al_{13} polycations (3.5 and 64.1 ppm, ref. Table 1). A further difference being the fact that the ^{27}Al MAS NMR spectrum after heating to 120 °C showed as well a resonance attributable to boehmite-like species (7.9 ppm, ref. Table 1).

First, the presence of Al_{13} polycations will be addressed. It was shown by Schönherr et al. [44], who analyzed the thermal evolution of $Al_{13}O_{40}$-chloride, that the presence of Al_{13} polycations leads to an exothermic peak at ~800 °C. As this peak is indicative of eta-Al_2O_3 formation [34,41,42], one can conclude that the mere presence of Al_{13} results in the formation of eta-Al_2O_3. However, taking into account Tsuchida and co-workers [34,41] and Steinike et al. [42] according to whom the presence of amorphous alumina is the prerequisite for eta-Al_2O_3 formation, it cannot be ruled out that during thermal evolution, Al_{13} polycations together with other components of the samples transform into an amorphous intermediate, which as a result might be the paramount reason for the observed eta-Al_2O_3 formation. This assumption is supported by two facts. After heating to 500 °C, Al_{13} polycation containing xerogels were (i) X-ray amorphous (XRD pattern not shown), and (ii) showed ^{27}Al MAS NMR resonances of five-fold coordinated aluminum, usually being attributed to amorphous aluminas [12,26,27,30] (ref. Fig. 1, x500-pH3.4).

The above-mentioned presence of boehmite-like species (after heating to 120 °C) in group(iii) xerogels which poses a difference to group(ii) samples but represents a similarity with group(i) xerogels, arouses the question why these xerogels do not show a boehmite-like thermal evolution behavior as observed in group(i). One might explain the absence of a boehmite-like DTA pattern with a parallel transformation of boehmite-like xerogel parts along with amorphous ones as well as Al_{13} polycations. While the detected boehmite-like xerogel parts transform into alpha-Al_2O_3 via the intermediate formation of gamma-Al_2O_3, the amorphous xerogel parts and Al_{13} polycations undergo a transformation into alpha-Al_2O_3 via the formation of eta-Al_2O_3. This assumption can be discarded as will be illustrated in the following.

It was mentioned above that Misra [38] distinguishes crystalline and gelatinous boehmite. According to Souza Santos et al. [36] the transformation of gelatinous boehmite into alpha-Al_2O_3 can either take place via the intermediate formation of gamma-Al_2O_3 or eta-Al_2O_3. Hence, one might as well assume that instead of gamma-Al_2O_3-forming gelatinous boehmite group(iii) samples contain eta-Al_2O_3 forming gelatinous boehmite. Differentiating between gamma-Al_2O_3 or eta-Al_2O_3 is a difficult task as even well expressed gamma-Al_2O_3 and eta-Al_2O_3 result in almost identical XRD patterns [43]. However, according to Zhou and Snyder [43] gamma-Al_2O_3 transforms slower into alpha-Al_2O_3 than eta-Al_2O_3. Such a difference in transformation kinetics could indeed be detected. After heating to 1150 °C, a group(iii) xerogel observing a presumably eta-Al_2O_3 formation related exothermic DTA peak between 800 and 900 °C (Fig. 2, x120-pH3.4), only shows one distinct ^{27}Al MAS NMR resonance at 13.9 ppm (Fig. 1, x1150-pH3.4), attributable to alpha-Al_2O_3. In contrast to this sample, not only alpha-Al_2O_3 but also residues of transition alumina, were detected after heating to 1150 °C in a group(i), pseudo-boehmite xerogel sample (x1150-pH4.9). The presence of residues of transition alumina in the latter sample was deduced from ^{27}Al MAS NMR resonances at 8.2 ppm (Fig. 1, x1150-pH4.9) and XRD reflections assignable to theta-Al_2O_3 (Fig. 4, x1150-pH4.9).

If the boehmite-like xerogel parts in group(iii) xerogels were similar to the gamma-Al_2O_3 forming pseudo-boehmite detected in group(i), one would have expected to find — after heating to 1150 °C — in group(iii) sample x1150-pH3.4 a similar ^{27}Al MAS NMR resonance at 8.2 ppm, as in the group(i) sample x1150-pH4.9 (Fig. 1). On the contrary, no such resonance was found in group(iii) xerogel sample x1150-pH3.4, but a resonance at 13.9 ppm only, indicating the sole presence of alpha-Al_2O_3. As a result it can be concluded, that based on the distinction made by Souza Santos et al. [36], the boehmite-like species detected after heating to 120 °C in group(iii) samples can be assigned to gelatinous boehmite forming eta-Al_2O_3 instead of gelatinous boehmite forming gamma-Al_2O_3 (possibly being present in group(i) samples). Thus, it is rather unlikely that a parallel transformation of gamma-Al_2O_3 into alpha-Al_2O_3 along with Al_{13} polycations and amorphous species, as assumed above, takes place in group(iii) xerogels.

It is interesting to note that according to the results of Souza Santos et al. [36], shorter boehmite fibrils transform into alpha-Al_2O_3 via the intermediate formation of eta-Al_2O_3 whereas longer boehmite fibrils transform into alpha-Al_2O_3 via the intermediate formation of gamma-Al_2O_3. It is a possible consequence of the results reported by Souza Santos et al. [36] that the presence of eta-Al_2O_3 forming gelatinous boehmite in group(iii) xerogels implies that these xerogels contain shorter boehmite fibrils as the gamma-Al_2O_3 forming pseudo-boehmite in group(i). In this case, the formation of longer boehmite fibrils would have been suppressed in the parent sols of group(iii) xerogels, having a pH value between 3.2 and 4.2. Suppression of boehmite particle growth might be facilitated by Al_{13} polycations. In [16], the influence of aluminum speciation on particle shape was analyzed. These authors surmised that Al_{13} polycations might prevent the change from spherical to chainlike particle shape. A similar assumption was made by Assih et al. [40] who argued that boehmite sols were stabilized by the

presence of Al_{13} polycations which bound onto the surface of boehmite particles. Since group(iii) xerogels do show ^{27}Al MAS NMR resonances attributable to Al_{13} polycations these species might indeed be held responsible for the presumable stabilization of shorter boehmite fibrils during the sol to xerogel transition in group(iii) xerogels.

4.4. Phase transformation temperatures

For understanding the phase transformation of xerogels apart from pH value of the parent sols, NO_3^-/Al molar ratio plays an important role as well. Peak temperature of the presumably eta-Al_2O_3 formation related exothermic peak between 800 and 900 °C seems to be rather influenced by NO_3^-/Al molar ratio than by pH value. As can be seen in Fig. 3, peak temperature decreased with decreasing NO_3^-/Al molar ratio but appears to be unaffected by changing pH values as is illustrated in the encircled region in which pH values range between 1.0 and 2.8, whereas peak temperatures vary between 894 and 880 °C. The dominating role of NO_3^-/Al molar ratio on peak temperature is illustrated in samples A and B having comparable pH values but different NO_3^-/Al molar ratios. Both samples show markedly different presumably eta-Al_2O_3 related transformation temperatures. While sample B, having a molar ratio of $NO_3^-/Al = 1.2$ shows an exothermic peak at 877 °C, sample A, having a molar ratio of $NO_3^-/Al = 0.5$, transforms into eta-Al_2O_3 at 800 °C.

Another aspect concerns the influence of particle size on temperature of phase transformations. Such effects are discussed for $BaTiO_3$ [45], $PbTiO_3$ [46] and alpha-Al_2O_3 formation from 'pure' boehmites [47]. To the best of our knowledge, there are no literature reports regarding the influence of particle size on the formation temperature of eta-Al_2O_3 resulting from amorphous precursors containing mixtures of different AlO_x species. However, one might suspect that varying NO_3^-/Al molar ratio between $NO_3^-/Al \sim 0.4$ and $NO_3^-/Al = 3.0$ provokes a change in particle size which in turn might be the reason for the observed decrease in peak temperature of the presumably eta-Al_2O_3 formation related DTA peak between 800 and 900 °C (ref. Fig. 2). This assumption is unlikely as will be illustrated in the following. X-ray diffraction reflexes have the same broad appearance if samples with different NO_3^-/Al molar ratios ($NO_3^-/Al = 2.3$, Fig. 4; $NO_3^-/Al = 0.6$, not shown in this work) within the questionable range were analyzed. As a result, one might assume that these samples contain particles with the same small 'nanoform' particle size. Furthermore, similar reflexes together with TEM results of comparable sol–gel samples are shown in [35]. The comparable broad XRD reflexes found in this work suggest that NO_3^-/Al molar ratio does not have a major influence on particle size. Besides, as was shown in Fig. 2, aluminum nitrate in its as-received state with crystal sizes in the millimeter range yielded comparable DTA peak temperatures like xerogel x120-pH2.7 ($NO_3^-/Al = 2.3$, ref. Table 2) which, according to a previous study [16], originates from a sol having a particle size below 40 nm. Hence, changes in particle sizes do not seem to be the primary reason for the observed changes in DTA peak temperature between 800 and 900 °C. As a result, instead of assigning the observed changes in peak temperature between 800 and 900 °C to particle size effects, these changes should rather be attributed to differing chemical properties, i.e., most likely NO_3^-/Al molar ratio, of the xerogels. As the observed shift in peak temperature corresponds with changing NO_3^-/Al molar ratio, the observed shift in peak temperature might be related to a retarding effect of nitrate species onto phase transformation. As was shown with MS, a small but discernible nitrate release was detected at temperatures as high as 875 °C (ref. Table 3). A similar assumption has been made earlier by Wood et al. [13]. These authors, who also detected an eta-Al_2O_3 transformation peak via DTA, reported the release of chloride to coincide with eta-Al_2O_3 transformation. Samples without such a marked mass loss at the eta-Al_2O_3 transformation temperature observed a lower transformation temperature.

5. Conclusions

- A modified Yoldas procedure was used to prepare various aluminas which differ with respect to aluminum speciation and phase transformation behavior which, to a certain degree, allows the tailoring of desired xerogel composition.
- Conditions chosen for sol preparation (chemical composition, pH) also determine the aluminum speciation in solid products obtained after thermal treatments of gels obtained from these sols.
- Al_{13} polycations play a decisive role for thermally induced transformations from amorphous products via eta-Al_2O_3 to alpha-Al_2O_3 as they seem to stabilize shorter boehmite fibrils.

Acknowledgments

The financial support of the Deutsche Forschungsgemeinschaft (DFG) is gratefully acknowledged. The authors thank A. Marek, W. Altenburg and H. Marx for technical assistance.

References

[1] J. Čejka, Appl. Catal. A 254 (2003) 327.
[2] L. Shaw, R. Abbaschian, J. Am. Ceram. Soc. 78 (1995) 3376.
[3] R. Hauk, G.H. Frischat, K. Ruppert, Glass Sci. Technol. 72 (1999) 386.
[4] Y. Kobayashi, T. Ishizaka, Y. Kurokawa, J. Mater. Sci. 40 (2005) 263.
[5] T. Maki, S. Sakka, J. Non-Cryst. Solids 100 (1988) 303.
[6] B.E. Yoldas, Am. Ceram. Soc. Bull. 54 (1975) 289.
[7] L.F. Nazar, L.C. Klein, J. Am. Ceram. Soc. 71 (1988) 85.

[8] A.C. Pierre, D.R. Uhlmann, Mater. Res. Soc. Symp. Proc. 32 (1984) 119.
[9] F.W. Dynys, M. Ljungberg, J.W. Halloran, Mater. Res. Soc. Symp. Proc. 32 (1984) 321.
[10] Y. Kurokawa, T. Suga, S. Nakata, T. Ikoma, S. Tero-Kubota, J. Mater. Sci. Lett. 17 (1998) 275.
[11] J.Y. Bottero, M. Axelos, D. Tchoubar, J.M. Cases, J.J. Fripiat, F. Fiessinger, J. Colloids Interface Sci. 117 (1987) 47.
[12] G. Fu, L.F. Nazar, A.D. Bain, Chem. Mater. 3 (1991) 602.
[13] T.E. Wood, A.R. Siedle, J.R. Hill, R.P. Skarjune, C.J. Goodbrake, Mater. Res. Soc. Symp. Proc. 180 (1990) 97.
[14] C.J. Brinker, G.W. Scherer, Sol Gel Science—The Physics and Chemistry of Sol–Gel Processing, Academic Press, San Diego, CA, 1990, p. 59.
[15] D.E. Clark, W.J. Dalzell Jr., B.L. Adams, US-Patent 4,801,399, 1989.
[16] M. Dressler, M. Nofz, M. Gemeinert, J. Sol–Gel Sci. Technol. 38 (2006) 261.
[17] M. Nofz, J. Pauli, M. Dressler, C. Jäger, W. Altenburg, J. Sol–Gel Sci. Technol. 38 (2006) 25.
[18] L. Allouche, C. Huguenard, F. Taulelle, J. Phys. Chem. Solids 62 (2001) 1525.
[19] K. Shafran, O. Deschaume, C.C. Perry, Adv. Eng. Mater. 6 (2004) 836.
[20] D. Coster, A.L. Blumenfeld, J.J. Fripiat, J. Phys. Chem. 98 (1994) 6201.
[21] K. Sohlberg, S.T. Pantelides, S.J. Pennycook, J. Am. Chem. Soc. 123 (2001) 26.
[22] S. Acosta, R.J.P. Corriu, D. Leclercq, P. Lefèvre, P.H. Mutin, A. Vioux, J. Non-Cryst. Solids 170 (1994) 234.
[23] J. Aguado, J.M. Escola, M.C. Castro, B. Paredes, Microporous Mesoporous Mater. 83 (2005) 181.
[24] Römpp online, 〈http://www.roempp.com/prod/index1.html〉 (accessed 22.01.2006), searchword: 'Aluminiumnitrat'.
[25] L.F. Nazar, D.G. Napier, D. Lapham, E. Epperson, Mater. Res. Soc. Symp. Proc. 180 (1990) 117.
[26] K.J.D. MacKenzie, J. Temuujin, M.E. Smith, P. Angerer, Y. Kameshima, Thermochim. Acta 359 (2000) 87.
[27] J.J. Fitzgerald, G. Piedra, S.F. Dec, M. Seger, G.E. Maciel, J. Am. Chem. Soc. 119 (1997) 7832.
[28] A. Vargas, J.A. Montoya, C. Maldonado, I. Hernández-Pérez, D.R. Acosta, J. Morales, Microporous Mesoporous Mater. 74 (2004) 1.
[29] B.C. Schmidt, F. Gaillard, M.E. Smith, Solid State Nucl. Magn. Res. 26 (2004) 197.
[30] G.K. Fandrei, T.J. Bastow, J.S. Hall, C. Jäger, M.E. Smith, J. Phys. Chem. 99 (1995) 15138.
[31] W. Deng, P. Bodart, M. Pruski, B.H. Shanks, Microporous Mesoporous Mater. 52 (2002) 169.
[32] The International Centre for Diffraction Data (ICDD), Powder Diffraction File PDF4+, card 43-1484, 2005.
[33] The International Centre for Diffraction Data (ICDD), Powder Diffraction File PDF4+, card 21-1307, 2005.
[34] T. Tsuchida, N. Ichikawa, React. Solids 7 (1989) 207.
[35] M. Nofz, R. Stösser, G. Scholz, I. Dörfel, J. Eur. Ceram. Soc. 25 (2005) 1095.
[36] P. Souza Santos, H. Souza Santos, S.P. Toledo, Mater. Res. 3 (2000) 104.
[37] W.A. Yarbrough, R. Roy, J. Mater. Res. 2 (1987) 494.
[38] C. Misra, Industrial alumina chemicals, Am. Chem. Soc. (1986) 8.
[39] M. Nguefack, A.F. Popa, S. Rossignol, C. Kappenstein, Phys. Chem. Chem. Phys. 5 (2003) 4279.
[40] T. Assih, A. Ayral, M. Abenoza, J. Phalippou, J. Mater. Sci. 23 (1988) 3326.
[41] T. Tsuchida, Thermochim. Acta 231 (1994) 337.
[42] U. Steinike, H. Geissler, H.P. Hennig, K. Jancke, J. Jedamzik, U. Kretzschmar, Z. Anorg. Allg. Chem. 590 (1990) 213.
[43] R.S. Zhou, R.L. Snyder, Acta Crystallogr. B 47 (1991) 617.
[44] S. Schönherr, H. Görz, D. Müller, W. Gessner, Z. Anorg. Allg. Chem. 476 (1981) 188.
[45] P. Perriat, J.C. Niepce, G. Caboche, J. Therm. Anal. 41 (1994) 635.
[46] C.J. Lu, H.M. Shen, Y.N. Wang, Mater. Lett. 34 (1998) 5.
[47] M.L. Guzmán-Castillo, X. Bokhimi, A. Toledo-Antonio, J. Salmones-Blásquez, F. Hernández-Beltrán, J. Phys. Chem. B 105 (2001) 2099.